Hierarchical Divergence-Conforming Vector Bases for Pyramid Cells

Hierarchical Divergence-Conforming Vector Bases for Pyramid Cells

Roberto D. Graglia, *Life Fellow, IEEE*

***Abstract*—Divergence-conforming hierarchical vector bases for the pyramid consist of face- and volume-based functions obtained by a simple procedure that uses a new paradigm recently introduced by this author to produce pyramid bases. In order to define the bases' order, the procedure starts by mapping the pyramids into a cube of a new Cartesian space, which we call the grandparent space, where the basis functions and their divergences take on polynomial form. Then we get the face-based functions of zero polynomial order and the volume-based functions of the first order. Functions of arbitrarily high order are obtained by multiplying the vector functions of the lowest order by independent scalar polynomials of higher order. Our face-based functions conform to those of other differently shaped elements to allow the use of hybrid meshes, while the multiplicative construction technique generates right away the volume-based basis functions. The completeness of the bases is demonstrated and all the basis functions we obtain are suitably normalized; their expression involves orthogonal polynomials which are easy to implement and alleviate the loss of linear independence**

***Index Terms* – Electromagnetic fields, finite-element methods, higher order vector elements, pyramidal elements, numerical analysis.**

I. Introduction

Successful three-dimensional (3D) electromagnetic codes must be able to model complicated geometries using higher-order vector basis functions on all four types of geometrical shapes: tetrahedra, hexahedron (bricks), prisms, and pyramids. As illustrated in [1], a conceptually simple method for constructing vector bases of polynomial order p for tetrahedral, brick and prismatic cells is to take the product of the zeroth-order basis vectors of the Nédélec type [2] with a set of scalar polynomials complete to the p-th order, to obtain a set of vector functions of the Nédélec type; the base is then extracted from this set by eliminating any redundancy, that is all dependent functions. The curl- (divergence-) conforming bases thus obtained are complete to the p-th order if able to represent any vector of polynomial order p, and if the curl (divergence) of any vector of order $(p+1)$, yielding a vector (scalar) of order p, can always be expressed as a linear combination of the curl (divergence) of such bases. Hence, when complete, our bases span the mixed-order spaces of Nédélec [2] (some-times known as *reduced gradient* spaces for curl-conforming functions). The complete hierarchical and interpolatory bases reported in [1] were all constructed using this multiplicative construction method, and are associated with a De Rham exact discretized sequence.

Despite this, unfortunately, there is still no generally accepted method that works equally well on pyramids, that is on cells with four triangular faces and one quadrilateral face. On the contrary, the few methods so far introduced in [3]-[11] to build the pyramidal bases require specialized knowledge and skills to be understood and have produced higher-order bases different from each other. Although the literature on this topic is not consolidated, as already discussed in the Introduction of [12], the results in [10] nevertheless deserve particular attention.

The main merit of [10] is to constuct bases in such a way that they describe finite-dimensional subspaces associated with a De Rham exact discretized sequence. In particular, *for pyramids,* this leads to subdividing the volume-based divergence- (curl-) conforming functions into different families of functions, that is those with zero divergence (curl) and others with non-zero divergence (curl). This obviously cannot be obtained with a multiplicative construction technique like ours, and it is of little use if one wants to obtain interpolatory bases such those in [1]. For our purposes, the main result of [10] is the number of volume-, face-, and edge-based functions associated with a pyramid cell (the edge-based are needed only to build curl-conforming bases); numbers that are identical to those we find for our bases obtained with the multiplicative technique.

The relatively small amount of existing literature along with the complex construction of the pyramid bases becomes annoying when one is forced to use pyramids to apply an adaptive technique; pyramids are in fact the natural *fillers* for hybrid meshes made up of a mixture of tetrahedra, brick and prismatic cells [5]. At the same time, there is also a lot of interest in increasing the order of the elements, whatever their shape, because

1) models that use higher-order elements use fewer degrees

Manuscript received August 22, 2022; revised December 14, 2022; accepted January 15, 2023. This work was supported by the European Union – Next Generation EU within the PNRR project *"Multiscale modeling and Engineering Applications"* of the Italian National Center for HPC, Big Data and Quantum Computing and, in part, by the Italian Ministry of University and Research (MUR) under PRIN Grant 2017NT5W7Z. *(Corresponding author: Roberto D. Graglia.)*

R.D. Graglia is with the Dipartimento di Elettronica e Telecomunicazioni (DET), Politecnico di Torino, Corso Duca degli Abruzzi 24, 10129 Torino, Italy (email: roberto.graglia@polito.it).

of freedom (DoF), i.e., fewer unknowns [1];
2) sophisticated parallel solution strategies can benefit from the use of higher-order elements [13];
3) mesh refinement occurs more naturally when the mesh cells are defined by higher order shape functions;
4) h- or p-adaptive techniques provide faster convergence as the order of the elements increases [14], [15], [16].

Given the growing interest in hybrid models that use differently shaped cells, and in consideration of all the difficulties encountered so far in building conforming higher-order pyramids, the new paradigm recently proposed in [12] seems to be a turning point as it allows to easily produce higher order pyramidal bases having simple and easily implementable expressions. Indeed, [12] discusses in depth new *hierarchical curl-conforming* bases for the pyramid that complement and are compatible with the families reported in [1], with continuous tangential components across adjacent cells in the mesh; that is, the families first presented individually in [17], [18], [19]. Similarly, the present article uses the same paradigm as [12] to build *hierarchical divergence-conforming* bases for pyramids that complement the families reported in [20] (as well as in [1]), with continuous normal components across adjacent cells in the mesh.

The basis functions presented here avoid spurious modes and solutions because divergence-conforming. They are constructed from orthogonal polynomials by a process similar to that used to generate the vector bases in [20], and are shown to alleviate the loss of linear independence. As regards spurious modes and solutions, we recall in passing that they are encountered every time the null space of the operator at issue is badly approximated, for example when using scalar representations with the common equations describing electromagnetic fields, specifically the integral equations (electric-field, magnetic-field and combined-field), the curl-curl form of the Helmholtz vector equation, and the first-order Maxwell's equations. In this regard, we may observe that the literature on spurious solutions of integral equations is not as extensive as that in the context of the Finite Element Method (FEM), due to the ease of implementation of the divergence-conforming functions normally used for the solution of surface integral equations, such as the zero-order RWG functions, which have been around for more than 40 years [21], or the higher order GWP basis functions, published more than 25 years ago [22].

As said, a brief historical review of research devoted to the development of basis functions for pyramidal cells can be found in the Introduction of [12]. Here we just reiterate that, in our opinion, the main problem that researchers have had so far in building the bases for the pyramid is to find the simplest and most direct way to build the volume-based vector functions that here, as in [12], we get thanks to simple analytical and geometric considerations. The divergence-conforming face-based functions are in fact derived from the known expression of the face-based functions of the remaining elements of different shape that may have a triangular or quadrilateral face

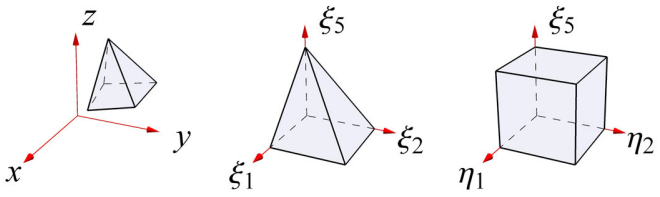

Fig. 1. Child pyramids are all obtained by mapping onto the observer's space a single parent pyramid through suitable shape functions. The figure shows a child pyramid on the left and the parent pyramid in the center. Shape and basis functions take polynomial form in the grandparent space ($\boldsymbol{\eta}$, ξ_5) where the pyramid domain is the unit cube shown on the right.

in common with the pyramid (so to speak, by imposing the normal continuity at the boundary of the cell).

The remainder of the paper is structured as follows. Section II reviews the different spaces and variables introduced to describe the pyramidal elements. Section III presents the lowest order base given in [5] and its main properties. Fundamental, first-order volume-based functions are discussed in Section IV and higher-order bases are presented in Section V. Numerical results are provided in Section VI. Readers may find it helpful to review [5], [12] for a detailed introduction to the notation and other background information. Preliminar results of this work were presented in [23].

II. Pyramid Geometry Representations

A pyramid is described using five *parent* variables $\{\xi_1, \xi_2, \xi_3, \xi_4, \xi_5\}$ and its faces are numbered to match the indexing of the associated parametric coordinate [5], [12]; that is, the i-th face of the pyramid is the zero-coordinate surface for the normalized coordinate ξ_i. More specifically, with reference to Fig. 1, the fifth face with parametric equation $\xi_5 = 0$ is always quadrilateral, the remaining four triangular faces have equation $\xi_j = 0$, for j from 1 to 4. We choose as *independent* coordinates ξ_1, ξ_2 and ξ_5, so that $\boldsymbol{\nabla}\xi_5 \cdot (\boldsymbol{\nabla}\xi_1 \times \boldsymbol{\nabla}\xi_2)$ is strictly positive, while ξ_3 and ξ_4 are *dependent* coordinates. The dependency relations in the parent space are [5], [12]

$$\begin{aligned} \xi_1 + \xi_3 + \xi_5 &= 1, \\ \xi_2 + \xi_4 + \xi_5 &= 1. \end{aligned} \tag{1}$$

In addition to the parent space, it is convenient to define and work in the *grandparent* space obtained by introducing the four *scaled* coordinates [10], [12]

$$\eta_j = \frac{\xi_j}{1-\xi_5} \tag{2}$$

$$\boldsymbol{\nabla}\eta_j = \frac{\boldsymbol{\nabla}\xi_j + \eta_j \boldsymbol{\nabla}\xi_5}{1-\xi_5} \tag{3}$$

with $j = 1, 2, 3, 4$. The coordinate ξ_5 remains an independent coordinate of the grandparent space. In this case, for $\xi_5 \neq 1$, the dependency relations (1) become

$$\eta_1 + \eta_3 = 1; \quad \eta_2 + \eta_4 = 1. \tag{4}$$

TABLE I: NODAL SHAPE FUNCTIONS FOR THE PYRAMID, FROM [5]

Interpolation Point		First Order Shape Functions
base corner	(4)	$(1-\xi_5)\eta_i\eta_{i+1}$
tip	(1)	ξ_5
		Second Order Shape Functions
base corner	(4)	$(1-\xi_5)\eta_i\eta_{i+1}\left[(2\eta_i-1)\right.$ $\left.(2\eta_{i+1}-1)(1-\xi_5)-\xi_5\right]$
base edge midpoint	(4)	$4(1-\xi_5)^2\,\eta_{i+1}\eta_{i-1}\,\eta_i\,(2\eta_i-1)$
base middle node	(1)	$16\,(1-\xi_5)^2\eta_1\eta_2\eta_3\eta_4$
lateral edge midpoint	(4)	$4\,\eta_i\eta_{i+1}\xi_5(1-\xi_5)$
tip	(1)	$\xi_5\,(2\xi_5-1)$

With subscripts counted modulo 4, for $i=1,4$

This Table reports the interpolatory first and second order shape functions of [5, Table I] associated respectively with 5 and 14 interpolation points. To clarify to the reader how these functions are used let us consider, with reference to Fig. 1, the five first-order shape functions that map the grandparent cube onto the pyramid of the observer's space as follows

$$\begin{aligned}\boldsymbol{r}(\eta_1,\eta_2,\eta_3,\eta_4,\xi_5) \quad &= \quad (1-\xi_5)\,(\eta_1\eta_2\boldsymbol{r}_{12}+\eta_2\eta_3\boldsymbol{r}_{23}\\ &\quad +\eta_3\eta_4\boldsymbol{r}_{34}+\eta_4\eta_1\boldsymbol{r}_{41})+\xi_5\boldsymbol{r}_5\end{aligned}$$

with the constraints $\eta_1+\eta_3=1$, $\eta_2+\eta_4=1$, and with $\boldsymbol{r}_{ij}$ and $\boldsymbol{r}_5$ denoting the vertices of the pyramid in the observer space. Clearly this mapping is multilinear in the grandparent space, while each face of the pyramid is mapped by bilinear functions of the grandparent coordinates. However, going back to using parent coordinates, the parameterizations of the pyramid faces simplify as follows

$$\boldsymbol{r}_\Sigma=\begin{cases}\xi_2\boldsymbol{r}_{23}+\xi_4\boldsymbol{r}_{34}+\xi_5\boldsymbol{r}_5 & \text{on face } \eta_1=0,\xi_1=0\\ \xi_3\boldsymbol{r}_{34}+\xi_1\boldsymbol{r}_{41}+\xi_5\boldsymbol{r}_5 & \text{on face } \eta_2=0,\xi_2=0\\ \xi_4\boldsymbol{r}_{41}+\xi_2\boldsymbol{r}_{12}+\xi_5\boldsymbol{r}_5 & \text{on face } \eta_3=0,\xi_3=0\\ \xi_1\boldsymbol{r}_{12}+\xi_3\boldsymbol{r}_{23}+\xi_5\boldsymbol{r}_5 & \text{on face } \eta_4=0,\xi_4=0\\ \xi_1\xi_2\boldsymbol{r}_{12}+\xi_2\xi_3\boldsymbol{r}_{23}+ & \\ \quad+\xi_3\xi_4\boldsymbol{r}_{34}+\xi_4\xi_1\boldsymbol{r}_{41} & \text{on face } \xi_5=0\end{cases}$$

Above we have a first order mapping because each triangular face is parameterized linearly by its area coordinates $\xi_{i+1},\xi_{i-1},\xi_5$, with $\xi_{i+1}+\xi_{i-1}+\xi_5=1$, using the three corner nodes of the face as interpolation points (the interpolation points for the quadrilateral face are its four corner nodes). Similarly, when mapping with second-order shape functions, we use 6 interpolation points on each triangular face and 9 on the quadrilateral base of the pyramid, as is always the case for second-order parameterizations of triangular and quadrilateral faces.

and, in the grandparent space, the pyramid is a cubic cell [12]. Then, as shown in Fig. 1, the parent and the grandparent cell are mapped into the observer space (x,y,z) through the use of appropriate shape functions [5], [12] which are *polynomials* of the *grandparent variables*. Although the shape functions are beyond the scope of this paper, in Table I we report the interpolatory shape functions of [5] outlining the first order mapping, by way of example. In fact, to simplify the construction of hybrid "conforming" meshes, we find it more convenient to use interpolatory shape-functions as done in [1] for all other cells of different shapes (tetrahedrons, prisms and bricks), although we would not mind at all immediately using shape functions like those used in computer graphics (e.g. NURBS, or similar). This means that the shape functions we use must be interpolatory polynomials of 3 *parent* variables on each triangular face of the mesh, and of 4 *parent* variables on each quadrilateral face. In order for this to happen, bearing in mind that on each face one of the parent variables of the cell vanishes, the shape functions of the pyramid turn out to be *fractional* functions of the parent variables (see [5, Table I]) while, as shown here in Table I, they are *polynomials* of the grandparent variables. When using pyramidal fillers, the shape functions of Table I are in general sufficient because in most cases the faces are mapped by interpolatory polynomials of first or second degree; higher grade mappings are rarely needed.

III. THE ZEROTH-ORDER BASE AND THE BUBBLE IT HIDES

The pyramidal base of the lowest possible order is reported in [5] together with the proof of its completeness. For the reader's convenience, Table II summarizes the expressions and the main properties of this base, as well as the formulas for calculating the generally non-constant values of the Jacobian ($\mathcal{J}$), of the gradient vectors ($\boldsymbol{\nabla}\xi_a$), and of the edge vectors ($\boldsymbol{\ell}_{ab}$) of a pyramidal cell. Using the grandparent variables (see Fig. 1 on the right), the lambda functions of Table II are derived from the fractional functions provided in [5] by replacing each parent variable ξ_γ with $(1-\xi_5)\eta_\gamma$. The lambda functions of Table II form a *polynomial* base of *order zero* in the grandparent space

1) because in the grandparent space the singularities disappear and the lambdas have a polynomial and no longer fractional form as in [5];
2) because of the completeness identities reported in the second row on the right of Table II which prove that any constant vector of arbitrary direction is a linear combination of these functions, apart from the $1/\mathcal{J}$ factor;
3) because they are functions with constant divergence, apart from the factor $1/\mathcal{J}$;
4) because they have a non-zero constant normal (CN) component on the face identified by their subscript, with a zero normal component on the remaining faces.

To build higher order bases it is also important to emphasize that the zeroth-order functions

$$\boldsymbol{\Lambda}_\gamma(\boldsymbol{r})=\frac{\eta_{\gamma+2}}{\mathcal{J}}\boldsymbol{\ell}_{\gamma-1,5}-\boldsymbol{B}_0(\boldsymbol{r}) \tag{5}$$

contain a component

$$\boldsymbol{B}_0(\boldsymbol{r})=\xi_5\frac{\left(\eta_1\boldsymbol{\ell}^1+\eta_2\boldsymbol{\ell}^2-\boldsymbol{\ell}^5\right)}{2\mathcal{J}} \tag{6}$$

whose divergence

$$\boldsymbol{\nabla}\cdot\boldsymbol{B}_0(\boldsymbol{r})=\frac{1}{(1-\xi_5)\mathcal{J}}-\frac{3}{2\mathcal{J}} \tag{7}$$

is singular. $\boldsymbol{B}_0(\boldsymbol{r})$ is a bubble function, where by bubble we mean a divergence-conforming function with zero normal

TABLE II: PYRAMID'S GEOMETRY REPRESENTATION AND LOWEST ORDER DIVERGENCE-CONFORMING BASE

As already reported in [12, Table I], the element Jacobian ($\mathcal{J}$) and the *gradient vectors* ($\boldsymbol{\nabla}\xi_a$)

$$\mathcal{J} = \boldsymbol{\ell}^1 \cdot \boldsymbol{\ell}^2 \times \boldsymbol{\ell}^5$$

$$\boldsymbol{\nabla}\xi_5 = \frac{\boldsymbol{\ell}^1 \times \boldsymbol{\ell}^2}{\mathcal{J}}, \quad \boldsymbol{\nabla}\xi_1 = \frac{\boldsymbol{\ell}^2 \times \boldsymbol{\ell}^5}{\mathcal{J}}, \quad \boldsymbol{\nabla}\xi_2 = \frac{\boldsymbol{\ell}^5 \times \boldsymbol{\ell}^1}{\mathcal{J}},$$

$$\boldsymbol{\nabla}\xi_3 = -\left(\boldsymbol{\nabla}\xi_1 + \boldsymbol{\nabla}\xi_5\right), \qquad \boldsymbol{\nabla}\xi_4 = -\left(\boldsymbol{\nabla}\xi_2 + \boldsymbol{\nabla}\xi_5\right)$$

are expressed in terms of the *unitary basis vectors* $\boldsymbol{\ell}^1$, $\boldsymbol{\ell}^2$, $\boldsymbol{\ell}^5$ (generally different from constant) which are the derivatives of the element position vector $\boldsymbol{r}$ with respect to the *independent* coordinates ξ_1, ξ_2 and ξ_5. The element edges are formed by intersection of pairs of zero-coordinates surfaces, and the *edge vectors*

$$\boldsymbol{\ell}_{ab} = \mathcal{J}\, \boldsymbol{\nabla}\xi_a \times \boldsymbol{\nabla}\xi_b$$

are directed along the cross product of the associated coordinate gradients. The edges are given a two-index label deriving from the two coordinate indices appearing in this cross product. The *unitary basis vectors* determine the following eight *edge vectors*

$$\begin{aligned} \boldsymbol{\ell}_{25} = -\boldsymbol{\ell}_{45} &= \boldsymbol{\ell}^1 \qquad & \boldsymbol{\ell}_{23} &= \boldsymbol{\ell}^5 - \boldsymbol{\ell}^1 \\ \boldsymbol{\ell}_{35} = -\boldsymbol{\ell}_{15} &= \boldsymbol{\ell}^2 \qquad & \boldsymbol{\ell}_{34} &= \boldsymbol{\ell}^5 - \boldsymbol{\ell}^1 - \boldsymbol{\ell}^2 \\ \boldsymbol{\ell}_{12} &= \boldsymbol{\ell}^5 \qquad & \boldsymbol{\ell}_{41} &= \boldsymbol{\ell}^5 - \boldsymbol{\ell}^2 \end{aligned}$$

with $\boldsymbol{\ell}_{12}$, $\boldsymbol{\ell}_{23}$, $\boldsymbol{\ell}_{34}$, $\boldsymbol{\ell}_{41}$ oriented towards the tip of the pyramid and $\boldsymbol{\ell}_{15}$, $\boldsymbol{\ell}_{25}$, $\boldsymbol{\ell}_{35}$, $\boldsymbol{\ell}_{45}$ arranged counterclockwise when viewed from the tip of the pyramid. The *mixed edges* 15, 25, 35, 45 are in common with a triangular face and the quadrilateral face; the *triangle edges* 12, 23, 34, 41 are shared only by triangular faces.

By counting modulo 4 all the subscripts obtained by varying γ from 1 to 4, the (five) basis functions are

$$\begin{aligned} \boldsymbol{\Lambda}_\gamma(\boldsymbol{r}) &= \frac{\eta_{\gamma+2}}{\mathcal{J}} \boldsymbol{\ell}_{\gamma-1,5} - \boldsymbol{B}_0(\boldsymbol{r}) \\ \boldsymbol{\Lambda}_5(\boldsymbol{r}) &= \frac{(1-\xi_5)}{\mathcal{J}} \left(\eta_1 \boldsymbol{\ell}^1 + \eta_2 \boldsymbol{\ell}^2 - \boldsymbol{\ell}^5\right) \end{aligned}$$

with

$$\eta_\gamma = \frac{\xi_\gamma}{1-\xi_5}, \qquad (1-\xi_5)\boldsymbol{\nabla}\eta_\gamma = \boldsymbol{\nabla}\xi_\gamma + \eta_\gamma \boldsymbol{\nabla}\xi_5$$

and where

$$\boldsymbol{B}_0(\boldsymbol{r}) = \xi_5 \frac{\left(\eta_1 \boldsymbol{\ell}^1 + \eta_2 \boldsymbol{\ell}^2 - \boldsymbol{\ell}^5\right)}{2\mathcal{J}} = \frac{\xi_5}{2(1-\xi_5)} \boldsymbol{\Lambda}_5(\boldsymbol{r})$$

is a bubble function with vanishing normal component on all the faces of the pyramid, and singular divergence

$$\boldsymbol{\nabla} \cdot \boldsymbol{B}_0 = \frac{1}{\mathcal{J}} \left(\frac{1}{1-\xi_5} - \frac{3}{2}\right) = \frac{1}{\mathcal{J}} \left(\frac{1}{1-\xi_5}\right) - \boldsymbol{\nabla} \cdot \boldsymbol{\Lambda}_\gamma$$

The base completeness follows from the identities

$$\begin{aligned} \boldsymbol{\Lambda}_3(\boldsymbol{r}) - \boldsymbol{\Lambda}_1(\boldsymbol{r}) &= \boldsymbol{\ell}^1/\mathcal{J} \\ \boldsymbol{\Lambda}_4(\boldsymbol{r}) - \boldsymbol{\Lambda}_2(\boldsymbol{r}) &= \boldsymbol{\ell}^2/\mathcal{J} \\ \boldsymbol{\Lambda}_3(\boldsymbol{r}) + \boldsymbol{\Lambda}_4(\boldsymbol{r}) - \boldsymbol{\Lambda}_5(\boldsymbol{r}) &= \boldsymbol{\ell}^5/\mathcal{J} \end{aligned}$$

On curvilinear pyramids, completeness is with respect to these vectors as weighting factors. Completeness of the divergence to zeroth order with respect to $1/\mathcal{J}$ as a weighting factor follows from

$$\boldsymbol{\nabla} \cdot \boldsymbol{\Lambda}_\gamma(\boldsymbol{r}) = 3/(2\mathcal{J}) \qquad \boldsymbol{\nabla} \cdot \boldsymbol{\Lambda}_5(\boldsymbol{r}) = 3/\mathcal{J}$$

$\boldsymbol{\Lambda}_i$ has zero normal component on all faces of the pyramid except on face i where it has a non-zero constant normal (CN) component which matches with that of the divergence-conforming bases of adjacent elements, possibly of different shape. $\boldsymbol{\Lambda}_i$ can thus interpolate the vector component normal to the centroid of face i and is readily normalized by ensuring a unit component along the normal at the corresponding interpolation point. The normalized form of the zeroth order bases is $\mathcal{J}\boldsymbol{\Lambda}_i(\boldsymbol{r})/h_i$, where $h_i = 1/\left|\boldsymbol{\nabla}\xi_i\right|$ is the magnitude of the height vector $\boldsymbol{h}_i$ at the centroid of face i. Dependencies among higher order functions arise from linear combinations of the bases which contain one of the following identities as a factor

$$(1-\xi_5)\eta_1 \boldsymbol{\Lambda}_1 + (1-\xi_5)\eta_3 \boldsymbol{\Lambda}_3 + \xi_5\, \boldsymbol{\Lambda}_5/2 = \boldsymbol{0} \qquad (1-\xi_5)\eta_2 \boldsymbol{\Lambda}_2 + (1-\xi_5)\eta_4 \boldsymbol{\Lambda}_4 + \xi_5\, \boldsymbol{\Lambda}_5/2 = \boldsymbol{0}$$

component on all faces of the pyramid, that is a volume-based function. Now, by evaluating the divergence of (5) to get

$$\boldsymbol{\nabla} \cdot \boldsymbol{\Lambda}_\gamma(\boldsymbol{r}) = \frac{3}{2\mathcal{J}} \tag{8}$$

it can be observed that the divergence of $\boldsymbol{B}_0$ cancels the singularity of the divergence of the first component to the right of (5). Notice here that $\boldsymbol{B}_0$ cannot be represented by polynomial basis functions, nor can it be a basis function of a polynomial base due to the singularity in its divergence; yet, $\boldsymbol{B}_0$ is a component of as many as four basis functions of order zero. That said, by considering the expression of the divergence (7), and trying to increase the order of the functions, it is reasonable to expect $(1-\xi_5)\boldsymbol{B}_0$ to be a *polynomial* bubble. This is the case only if both $(1-\xi_5)\boldsymbol{B}_0$ and its divergence are polynomials (we establish the order of this bubble only after this has been verified). In fact we obtain

$$2(1-\xi_5)\boldsymbol{B}_0 = \xi_5 \boldsymbol{\Lambda}_5 \tag{9}$$

$$\boldsymbol{\nabla} \cdot [2(1-\xi_5)\boldsymbol{B}_0] = \boldsymbol{\nabla} \cdot [\xi_5 \boldsymbol{\Lambda}_5] = \frac{4\xi_5 - 1}{\mathcal{J}} \tag{10}$$

Since $\boldsymbol{\Lambda}_5$ is of order zero, $\xi_5 \boldsymbol{\Lambda}_5$ is a first order function with the linear (i.e., first order) divergence (10); therefore (9) is a first-order bubble.

To grow polynomial bases in a hierarchical way from zero to higher orders, and in particular to define the basis subset of bubble functions, we must introduce other *polynomial* bubbles beyond (9) that we construct, whatever their order, starting from the fundamental bubbles presented in the next Section.

IV. THE FUNDAMENTAL BUBBLES

Reiterating our intention to form polynomial vector bases in space $(\boldsymbol{\eta}, \xi_5)$, we observe that the lowest-order bubble functions we are interested in finding are those with linear divergence, since it is clear that there are no bubble functions with constant divergence other than zero. The lowest-order bubbles are identified by observing that on the left of the two equations

$$\begin{aligned} (1-\xi_5)\eta_1 \boldsymbol{\Lambda}_1 + (1-\xi_5)\eta_3 \boldsymbol{\Lambda}_3 + \xi_5\, \boldsymbol{\Lambda}_5/2 &= \boldsymbol{0} \\ (1-\xi_5)\eta_2 \boldsymbol{\Lambda}_2 + (1-\xi_5)\eta_4 \boldsymbol{\Lambda}_4 + \xi_5\, \boldsymbol{\Lambda}_5/2 &= \boldsymbol{0} \end{aligned} \tag{11}$$

reported at the bottom of Table II, we are adding up dependent functions. We can therefore consider the functions $(1-\xi_5)\eta_1\boldsymbol{\Lambda}_1$ and $(1-\xi_5)\eta_2\boldsymbol{\Lambda}_2$ as dependent on the three independent bubbles

$$(1-\xi_5)\eta_3\boldsymbol{\Lambda}_3, \quad (1-\xi_5)\eta_4\boldsymbol{\Lambda}_4, \quad 2(1-\xi_5)\boldsymbol{B}_0 \tag{12}$$

Using the definition (5) of $\boldsymbol{\Lambda}_\gamma$, we see that the two functions to the left of (12) contain the higher order bubbles $(1-\xi_5)\eta_3\boldsymbol{B}_0$ and $(1-\xi_5)\eta_4\boldsymbol{B}_0$ which we promptly remove, and this is the last step that, starting from (12), yields the three fundamental *bubbles* of the first order

$$\left[\begin{array}{c}\boldsymbol{\Lambda}_{B1}\\ \boldsymbol{\Lambda}_{B2}\\ \boldsymbol{\Lambda}_{B3}\end{array}\right] = \frac{(1-\xi_5)}{\mathcal{J}}\left[\begin{array}{c}\eta_3\eta_1\boldsymbol{\ell}^1\\ \eta_4\eta_2\boldsymbol{\ell}^2\\ \xi_5\left(\boldsymbol{\ell}^5-\eta_1\boldsymbol{\ell}^1-\eta_2\boldsymbol{\ell}^2\right)\end{array}\right] \tag{13}$$

with first-order divergence

$$\boldsymbol{\nabla}\cdot\left[\begin{array}{c}\boldsymbol{\Lambda}_{B1}\\ \boldsymbol{\Lambda}_{B2}\\ \boldsymbol{\Lambda}_{B3}\end{array}\right] = \frac{1}{\mathcal{J}}\left[\begin{array}{c}1-2\eta_1\\ 1-2\eta_2\\ 1-4\xi_5\end{array}\right] \tag{14}$$

The divergences (14) are special cases of the more general result

$$\boldsymbol{\nabla}\cdot\eta_1^\alpha\eta_2^\beta\xi_5^\delta\left[\begin{array}{c}\boldsymbol{\Lambda}_{B1}\\ \boldsymbol{\Lambda}_{B2}\\ \boldsymbol{\Lambda}_{B3}\end{array}\right] = \left[\begin{array}{c}(1+\alpha)-(2+\alpha)\eta_1\\ (1+\beta)-(2+\beta)\eta_2\\ (1+\delta)-(4+\delta)\xi_5\end{array}\right]\frac{\eta_1^\alpha\eta_2^\beta\xi_5^\delta}{\mathcal{J}} \tag{15}$$

which stems from the fact that the divergence of any linear combination of terms such as $\eta_1^\alpha\eta_2^\beta\xi_5^\delta(1-\xi_5)\boldsymbol{\ell}^a$ (where the superscript a in $\boldsymbol{\ell}^a$ is 1, 2, or 5) takes a polynomial form in the grandparent space $(\boldsymbol{\eta},\xi_5)$. (Of course, each term of these linear combinations can have different values of the exponents α, β, and δ.)

Equation (14) proves that $\boldsymbol{\Lambda}_{B1}$, $\boldsymbol{\Lambda}_{B2}$, $\boldsymbol{\Lambda}_{B3}$ belong to the same space and are of the same order, ie the first order. This result would not be so evident if we wrote these functions in terms of zero-order basis vectors, as follows

$$\left[\begin{array}{c}\boldsymbol{\Lambda}_{B1}\\ \boldsymbol{\Lambda}_{B2}\\ \boldsymbol{\Lambda}_{B3}\end{array}\right] = \left[\begin{array}{c}(1-\xi_5)\eta_3\eta_1\left(\boldsymbol{\Lambda}_3-\boldsymbol{\Lambda}_1\right)\\ (1-\xi_5)\eta_4\eta_2\left(\boldsymbol{\Lambda}_4-\boldsymbol{\Lambda}_2\right)\\ -\xi_5\boldsymbol{\Lambda}_5\end{array}\right] \tag{16}$$

V. Higher Order Bases

Higher-order hierarchical bases are obtained in a direct and clear way thanks to the new paradigm presented in [12] which for divergence-conforming sets is stated as follows

1) The vector components and the divergence of the basis functions are polynomials of the grandparent variables $\{\boldsymbol{\eta},\ \xi_5\}$. Unisolvency and base completeness must be proved in the grandparent space.
2) Each higher order vector function is obtained by multiplying one vector function of zero order, or a combination of zero order functions (as it happens for the fundamental bubbles of the previous Section), by a scalar generating polynomial which, in turn, is the product of normalized orthogonal polynomials (the same was done in [1], [20]).
3) The multiplicative polynomials are defined in the grandparent cubic cell of Fig. 1 (whose vertices are points of intersection of only three edges and faces).
4) On the pyramid border, the multiplicative polynomials that generate the face based functions coincide with those for the adjacent elements, no matter what shape they have.

Notice here that we can discuss on the order of the bases precisely because, or only when, the basis vectors are expressed in the grandparent space, which is precisely the only space in which they, together with their divergence, take on a polynomial expression. The basis vectors are defined using the orthogonal normalized sets of shifted Jacobi polynomials listed in Table III. Some of these sets have already been used elsewhere (for example in [12]) to form curl-conforming bases. The polynomials we use here are marked with a tilde on their symbol to avoid any possible confusion with the definitions given in previous articles.

According to our paradigm, for the face-based polynomial functions shown in Table IV it will be sufficient to demonstrate the continuity of the normal component through adjacent cells that may have different shapes, which we do in the following two sub-sections V.A and V.B. To this end, we recall that to ensure conformity, the face-based function straddling two adjacent cells must be oriented so as to have continuous normal component on the common face. Currently we guarantee that this happens only afterwards using the procedure explained in [20, Section III] and in [1] to adjust, if necessary, the sign of the face-based vector function on one of the two adjacent cells; the correct sign of the face-based functions can be embedded a priori in the expression of the functions with more sophisticated techniques.

A. Functions Based on Triangular Faces

For the pyramid, the divergence-conforming p-order complete set has a total of $2(p+1)(p+2)$ functions based on triangular faces because each zero-order function $\boldsymbol{\Lambda}_\gamma$ (for $\gamma=1$ to 4) generates $(p+1)(p+2)/2$ functions hierarchically organized as shown in the left column of Table IV. The multiplicative polynomials

$$F_{i0k}^\gamma = (1-\xi_5)^i\,\widetilde{A}_i(\eta_{\gamma+1})\,\widetilde{C}_k^{(i)}(\xi_5) \tag{17}$$

of Table IV which generate these functions can be written as follows

$$F_{i0k}^\gamma = Q_i(\xi_{\gamma+1},\xi_{\gamma-1})\,\widetilde{C}_k^{(i)}(\xi_5) \tag{18}$$

where $Q_i(\xi_{\gamma+1},\xi_{\gamma-1})$ is the normalized, shifted scaled Legendre polynomial defined in [12]. Expression (18) clarifies that, in the end, F_{i0k}^γ depends only on the variables used to parameterize face γ, namely the three face variables $\xi_{\gamma+1}$, $\xi_{\gamma-1}$, and ξ_5, with $\xi_5+\xi_{\gamma+1}+\xi_{\gamma-1}=1$. The polynomials F_{i0k}^γ do not depend at all on the three-dimensional shape of the cell

TABLE III: NORMALIZED ORTHOGONAL POLYNOMIALS USED TO BUILD DIVERGENCE-CONFORMING BASES

Normalized polynomial $\mathcal{P}_n(z)$	Normalization coefficient	Weight function
$\widetilde{A}_n(z) = N_a\, P_n^{(0,0)}(2z-1)$	$N_a = \sqrt{2n+1}$	1
$\widetilde{B}_n(z) = N_b\, P_n^{(2,2)}(2\,z-1)$	$N_b = \sqrt{\dfrac{(2n+5)(n+3)(n+4)}{(n+1)(n+2)}}$	$(1-z)^2\, z^2$
$\widetilde{C}_n^{(m)}(z) = N_c\, P_n^{(2m+1,0)}(2z-1)$	$N_c = \sqrt{2(m+n+1)}$	$(1-z)^{2m+1}$
$\widetilde{D}_n(z) = N_d\, P_n^{(4,0)}(2z-1)$	$N_d = \sqrt{2n+5}$	$(1-z)^4$
$\widetilde{E}_n(z) = N_e\, P_n^{(4,2)}(2z-1)$	$N_e = \sqrt{\dfrac{(2n+7)(n+5)(n+6)}{(n+1)(n+2)}}$	$(1-z)^4 z^2$

As already done for the other polynomials reported in [12, Table III], here too the polynomials $\mathcal{P}_n(z)$ in the left column are obtained by rescaling the shifted Jacobi polynomials $P_n^{(\alpha\beta)}(2z-1)$ of order n, being $P_n = P_n^{(00)}$ the Legendre polynomial. The system of polynomials $P_n^{(\alpha\beta)}(2z-1)$ is orthogonal on the interval $[0,1]$ with respect to the weight function $(1-z)^\alpha\, z^\beta$. The normalization coefficients depend on the order n of the polynomial itself, as well as on the value of the integer m that defines the exponent α of the corresponding weight function, reported in the right column for clarity. The polynomial systems listed in the left column satisfy the orthogonality relation

$$\int_0^1 w(z)\, \mathcal{P}_n(z)\, \mathcal{P}_\ell(z)\, \mathrm{d}z = \delta_{n\ell}$$

being $\delta_{n\ell}$ the Kronecker delta function. These polynomials have a zero derivative for $n = 0$, while for $n > 0$ we have

$$\frac{\mathrm{d}}{\mathrm{d}\,z}\,\widetilde{A}_n(z) \;=\; (n+1)\,N_a\,\frac{P_{n+1}(2z-1) - (2z-1)P_n(2z-1)}{2z(z-1)} \qquad \frac{\mathrm{d}}{\mathrm{d}\,z}\,\widetilde{D}_n(z) \;=\; (n+5)\,N_d\,P_{n-1}^{(5,1)}(2z-1)$$

$$\frac{\mathrm{d}}{\mathrm{d}\,z}\,\widetilde{B}_n(z) \;=\; (n+5)\,N_b\,P_{n-1}^{(3,3)}(2z-1) \qquad \frac{\mathrm{d}}{\mathrm{d}\,z}\,\widetilde{E}_n(z) \;=\; (n+7)\,N_e\,P_{n-1}^{(5,3)}(2z-1)$$

$$\frac{\mathrm{d}}{\mathrm{d}\,z}\,\widetilde{C}_n^{(m)}(z) \;=\; (2m+n+2)\,N_c\,P_{n-1}^{(2m+2,1)}(2z-1)$$

that rests on face γ, be it pyramidal, tetrahedral or triangular prism-shaped. (The names, or better, the subscripts associated with the parent variables $\{\xi_{\gamma+1}, \xi_{\gamma-1}, \xi_5\}$ may depend on the shape of the cell, but clearly this does not change the substance of things). Since F_{i0k}^γ does not depend on the three-dimensional shape of the cell, we can then recognize that, paying due attention to the names and order of the subscripts, the set (17) coincides with the polynomial set $F_{mn}(\boldsymbol{\xi}_t)$ given in [20, Table IV], except for a sign factor $(-1)^m$, with

$$(-1)^m\, F_{mn}(\boldsymbol{\xi}_t) = F_{n0m}^\gamma = Q_n(\xi_{\gamma+1}, \xi_{\gamma-1})\, \widetilde{C}_m^{(n)}(\xi_5) \quad (19)$$

$$\boldsymbol{\xi}_t = \{\xi_a, \xi_b, \xi_c\} = \{\xi_{\gamma+1}, \xi_{\gamma-1}, \xi_5\} \quad (20)$$

This occurs despite the fact that the $F_{mn}(\boldsymbol{\xi}_t)$ in [20, Table IV] have been obtained with an *ad hoc* technique, i.e. by orthogonalizing a polynomial set formed by the product of Legendre's polynomials. The sign of F_{i0k}^γ in Table IV (and of F_{n0m}^γ in (19)) is irrelevant because the continuity of the normal component of the vector basis function that straddles two adjacent cells having the triangular face in common is fixed a posteriori simply by adjusting the sign of this function in one of the two adjacent cells. In fact the polynomials F_{i0k}^γ are normalized as in [20] so that the integral of the square of F_{i0k}^γ on the triangular parent face $\xi_\gamma = 0$, i.e., on the simplex T^2, is equal to unity

$$\begin{aligned}\iint_{T^2} \left[F_{i0k}^\gamma(\boldsymbol{\xi}_t)\right]^2\, \mathrm{d}T^2 = \\ \int_0^1 \int_0^{1-\xi_5} \left[F_{i0k}^\gamma(\xi_{\gamma+1}, \xi_5)\right]^2\, \mathrm{d}\xi_5\, \mathrm{d}\xi_{\gamma+1} = \\ \int_0^1 \int_0^1 (1-\xi_5)\left[F_{i0k}^\gamma(\eta_{\gamma+1}, \xi_5)\right]^2\, \mathrm{d}\xi_5\, \mathrm{d}\eta_{\gamma+1} = 1\end{aligned} \quad (21)$$

B. Functions Based on the Quadrilateral Face

The divergence-conforming p-order complete set has a total of $(p+1)^2$ functions based on the quadrilateral face $\xi_5 = 0$ hierarchically organized as shown in the right column of Table IV. The zero-order function $\boldsymbol{\Lambda}_5$ that generates the higher order functions

$$\boldsymbol{\Lambda}_{ij0}^5 = F_{ij0}^5 \boldsymbol{\Lambda}_5 \quad (22)$$

$$\boldsymbol{\nabla} \cdot \boldsymbol{\Lambda}_{ij0}^5 = \frac{3}{\mathcal{J}} F_{ij0}^5 \quad (23)$$

contains the factor $(1-\xi_5)$, and this in any case would cancel the singularity in $\xi_5 = 1$ of the gradient of the multiplicative functions of Table IV

$$F_{ij0}^5 = \widetilde{A}_i(\eta_1)\, \widetilde{A}_j(\eta_2) \quad (24)$$

of global order $i + j$, with $0 \le i, j \le p$. Even better, in this case we get

$$\boldsymbol{\Lambda}_5 \cdot \boldsymbol{\nabla} F_{ij0}^5 = 0 \quad (25)$$

TABLE IV: THE DIVERGENCE-CONFORMING, FACE-BASED FUNCTIONS SUBSET OF ORDER p STRUCTURED IN HIERARCHICAL FORM

<table>
<tr>
<td>Functions Based on the Triangular Faces $\xi_\gamma = 0$

For $\gamma = 1$, 2, 3, and 4,
each $\mathbf{\Lambda}_\gamma$ generates $(p+1)(p+2)/2$ functions
$$\mathbf{\Lambda}^\gamma_{i0k} = F^\gamma_{i0k}\mathbf{\Lambda}_\gamma$$
$$\boldsymbol{\nabla}\cdot\mathbf{\Lambda}^\gamma_{i0k} = \frac{1}{2\mathcal{J}}\left[3\,F^\gamma_{i0k} + \widetilde{A}_i(\eta_{\gamma+1})\,G_{ik}(\xi_5)\right]$$
obtained for $i,k = 0,1,\ldots,p$ with $(i+k) = p$, and hierarchically organized as follows
• for $p = 0$ the set is made up of $\mathbf{\Lambda}^\gamma_{000}$;
• for $p \geq 1$, one has to increment the set of order $(p-1)$ with $(p+1)$ polynomials $\mathbf{\Lambda}^\gamma_{i0k}$ obtained for
$i = p-k, \quad k = 0$ to p.</td>
<td>Functions Based on the Quadrilateral Face $\xi_5 = 0$

$\mathbf{\Lambda}_5$ generates $(p+1)^2$ functions
$$\mathbf{\Lambda}^5_{ij0} = F^5_{ij0}\mathbf{\Lambda}_5$$
$$\boldsymbol{\nabla}\cdot\mathbf{\Lambda}^5_{ij0} = \frac{3}{\mathcal{J}}F^5_{ij0}$$
obtained for $i,j = 0,1,\ldots,p$, and hierarchically organized as follows
• for $p = 0$ the set is made up of $\mathbf{\Lambda}^5_{000}$;
• for $p \geq 1$, one has to increment the set of order $(p-1)$ with $(2p+1)$ polynomials $\mathbf{\Lambda}^5_{ij0}$ obtained for
$\Rightarrow i = p, \quad j = 0$ to p;
$\Rightarrow j = p, \quad i = 0$ to $p-1$.</td>
</tr>
<tr>
<td colspan="2">With $\quad F^\gamma_{i0k} = (1-\xi_5)^i\,\widetilde{A}_i(\eta_{\gamma+1})\,\widetilde{C}^{(i)}_k(\xi_5), \qquad F^5_{ij0} = \widetilde{A}_i(\eta_1)\,\widetilde{A}_j(\eta_2), \qquad \mathbf{\Lambda}_5\cdot\boldsymbol{\nabla}F^5_{ij0} = 0,$
$$G_{ik}(\xi_5) = \xi_5\,\frac{\mathrm{d}}{\mathrm{d}\xi_5}\left[(1-\xi_5)^i\,\widetilde{C}^{(i)}_k(\xi_5)\right] =$$
$$= \sqrt{2(i+k+1)}\,\xi_5\left\{-i(1-\xi_5)^{i-1}P^{(2i+1,0)}_k(2\xi_5-1) + (1-\xi_5)^i(2i+k+2)P^{(2i+2,1)}_{k-1}(2\xi_5-1)\right\}$$</td>
</tr>
</table>

On the face $\xi_5 = 0$, the polynomials (24) simplify into

$$F^5_{ij0}\big|_{\xi_5=0} = \sqrt{2i+1}\,\sqrt{2j+1}\,P_i(\xi_1-\xi_3)\,P_j(\xi_2-\xi_4) \quad (26)$$

and are therefore identical to the multiplicative polynomials used in [20] to define the functions based on quadrilateral faces, which demonstrates the continuity of the normal component on the face in common to the adjacent cell, be it a brick, a prism, or another pyramid.

C. Volume-Based Functions

In addition to the face-based functions of the previous subsections V.A and V.B, the divergence-conforming p-order complete set has a total of $3p(p+1)^2$ independent bubble functions hierarchically organized as shown in Table V. The number $3(\widetilde{p}-1)\widetilde{p}^{\,2}$ of volume-based functions in [10] coincides with the number of our bubbles by replacing $\widetilde{p}$ with $(p+1)$.

Ultimately, for a given order p, our pyramid and brick bases have the same number of independent bubbles, i.e., the same number of internal degrees of freedom (DoF). More precisely, for both the pyramid and the brick, the number of curl-conforming bubbles is $3p^2(p+1)$ [12] while, as said, the divergence-conforming families have $3p(p+1)^2$ bubbles.

D. Bases' Completeness

Completeness to order p in the divergence can be proved starting from (15). However, in this regard, it is much easier to observe that completeness is a direct consequence of the fact that the pyramid is mapped into a brick (i.e. the grandparent cube), and of the fact that the number of bubbles of a brick of order p is identical to what we obtained for the pyramid of the same order.

Likewise, completeness of the p-order vector base follows from the fact that the basis functions set contains all the *face-based* functions up to the p-order which can be defined on the bounding faces of the pyramid, plus all the volume-based functions up to the p-order which can be defined on a brick.

E. The First Order Base as an Example

The equality of the number of bubbles for the pyramid with that of the brick is not surprising when we consider that we have obtained these bases by working on a unitary cube. The space (parent or grandparent) in which this cube is located does not really matter. To clarify this, let us consider for a moment the bubble functions of the first-order base shown in Table VI, and in particular the divergence of these (here we do this for convenience, because the divergence is a scalar quantity, but the reasoning can be repeated for the vector components of the basis functions). The divergence of each bubble in Table VI is proportional to one of the scalar functions reported at the bottom of the same Table VI, and any linear, bilinear or trilinear function is certainly a linear combination of these scalar functions. As for divergence, the zero-order face-based functions and the linear bubbles of Table VI form a complete first-order set. To get the first-order complete *vector* set, we simply add to it the first-order face-based functions subset.

F. Number of Degrees of Freedom

The number of degrees of freedom for divergence-conforming bases of order p on a pyramid may be determined as follows:

- one component $\times((p+1)(p+2)/2)$ DOF's $\times$ four triangular faces plus one component $\times(p+1)^2$ DOF's

TABLE V: THE DIVERGENCE-CONFORMING, VOLUME-BASED FUNCTIONS SUBSET OF ORDER p STRUCTURED IN HIERARCHICAL FORM

We define the volume-based functions in terms of the following first-order bubbles with first-order divergence

$$\begin{bmatrix} \boldsymbol{\Lambda}_{B1} \\ \boldsymbol{\Lambda}_{B2} \\ \boldsymbol{\Lambda}_{B3} \end{bmatrix} = \frac{(1-\xi_5)}{\mathcal{J}} \begin{bmatrix} \eta_3\eta_1\boldsymbol{\ell}^1 \\ \eta_4\eta_2\boldsymbol{\ell}^2 \\ \xi_5\left(\boldsymbol{\ell}^5 - \eta_1\boldsymbol{\ell}^1 - \eta_2\boldsymbol{\ell}^2\right) \end{bmatrix}, \qquad \boldsymbol{\nabla}\cdot \begin{bmatrix} \boldsymbol{\Lambda}_{B1} \\ \boldsymbol{\Lambda}_{B2} \\ \boldsymbol{\Lambda}_{B3} \end{bmatrix} = \frac{1}{\mathcal{J}} \begin{bmatrix} 1-2\eta_1 \\ 1-2\eta_2 \\ 1-4\xi_5 \end{bmatrix}$$

There are $3p(p+1)^2$ independent bubble functions of polynomial order $(i+j+k)$

$$\begin{cases} \boldsymbol{\Lambda}_{ijk}^{B1} &= \widetilde{A}_i(\eta_2)\widetilde{D}_j(\xi_5)\widetilde{B}_{k-1}(\eta_1)\boldsymbol{\Lambda}_{B1} \\ \boldsymbol{\Lambda}_{ijk}^{B2} &= \widetilde{A}_i(\eta_1)\widetilde{D}_j(\xi_5)\widetilde{B}_{k-1}(\eta_2)\boldsymbol{\Lambda}_{B2} \\ \boldsymbol{\Lambda}_{ijk}^{B3} &= \widetilde{A}_i(\eta_1)\widetilde{A}_j(\eta_2)\widetilde{E}_{k-1}(\xi_5)\boldsymbol{\Lambda}_{B3} \end{cases}$$

$$\boldsymbol{\nabla}\cdot\boldsymbol{\Lambda}_{ijk}^{B1} = \frac{1}{\mathcal{J}}\widetilde{A}_i(\eta_2)\widetilde{D}_j(\xi_5)\left[(1-2\eta_1)\widetilde{B}_{k-1}(\eta_1) + (1-\eta_1)\eta_1\frac{\mathrm{d}}{\mathrm{d}\eta_1}\widetilde{B}_{k-1}(\eta_1)\right]$$

$$\boldsymbol{\nabla}\cdot\boldsymbol{\Lambda}_{ijk}^{B2} = \frac{1}{\mathcal{J}}\widetilde{A}_i(\eta_1)\widetilde{D}_j(\xi_5)\left[(1-2\eta_2)\widetilde{B}_{k-1}(\eta_2) + (1-\eta_2)\eta_2\frac{\mathrm{d}}{\mathrm{d}\eta_2}\widetilde{B}_{k-1}(\eta_2)\right]$$

$$\boldsymbol{\nabla}\cdot\boldsymbol{\Lambda}_{ijk}^{B3} = \frac{1}{\mathcal{J}}\widetilde{A}_i(\eta_1)\widetilde{A}_j(\eta_2)\left[(1-4\xi_5)\widetilde{E}_{k-1}(\xi_5) + (1-\xi_5)\xi_5\frac{\mathrm{d}}{\mathrm{d}\xi_5}\widetilde{E}_{k-1}(\xi_5)\right]$$

obtained for $i,j = 0,1,\ldots,p$ and $k = 1,\ldots,p$, and hierarchically organized as follows

- for $p=0$ there are no bubble functions;
- for $p=1$ the set contains 12 functions obtained by setting $\{ijk\} = \{001\}$, $\{101\}$, $\{011\}$, $\{111\}$,
- for $p \geq 2$, one has to increment the set of order $(p-1)$ with $3p(3p+1)$ polynomials with indices i,j, and k obtained for

$$\begin{array}{lll} i = p, & j = 0 \text{ to } p, & k = 1 \text{ to } p-1; \\ i = 0 \text{ to } p-1, & j = p, & k = 1 \text{ to } p-1; \\ i = 0 \text{ to } p, & j = 0 \text{ to } p, & k = p. \end{array}$$

$\times$ one quadrilateral face $= (p+1)(3p+5)$ face degrees of freedom.

- three components $\times p(p+1)^2$ DOF's $= 3p(p+1)^2$ interior degrees of freedom.

for a grand total of degrees of freedom per pyramid equal to

$$\text{DoF\#} = (p+1)(5+6p+3p^2) \tag{27}$$

Once again, by replacing p with $(\widetilde{p}-1)$, the grand total of DoF equals $3\,\widetilde{p}^3+2\,\widetilde{p}$ and agrees with the number of DoF previously determined in [10]. The number of DoF of the pyramid is always lower than that of the brick, while it remains higher than that of the triangular prism for $p \geq 1$ (see Fig. 2). Recall that pyramid and brick have the same number of interior DoF [1].

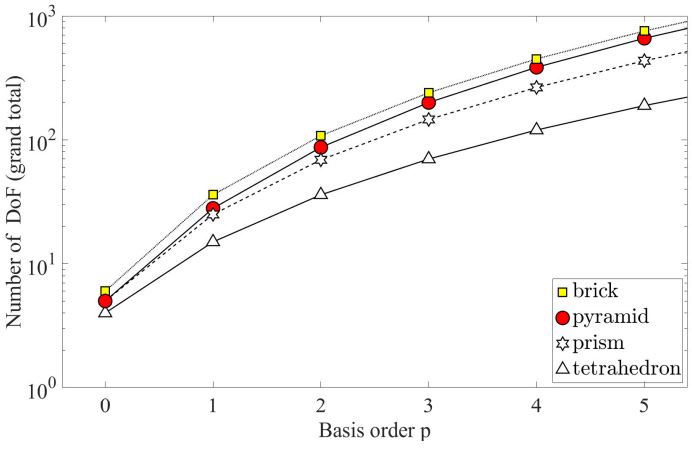

Fig. 2. Total number of degrees of freedom (DoF) for divergence-conforming vector bases of order p on single, differently shaped canonical cells.

VI. NUMERICAL RESULTS

Divergence conforming bases are usually employed in the numerical solution of integral equations via the Method of Moments (MoM). The main problem encountered in the use of hierarchical bases, not only the divergence-conforming but also the curl-conforming ones, is that the linear independence of the basis functions and the conditioning of the finite problems to be solved get worse as the order of the base increases [1]. In other words, the Condition Number (CN) of the system matrices obtained with the MoM tends to worsen as the order of the hierarchical base in use increases, although we have "injected", so to speak, some orthogonality into the set of the basis-functions precisely to guarantee a good control on the deterioration of the CN of the system matrices (by the way, this is more easily achieved using the Galerkin testing technique). In this regard, note that the advantages of using orthogonal bases are less evident in the solution of integral equations than those commonly found while numerically solving partial differential equations with orthogonal, curl-conforming bases. This happens because the discretization of integral equations involves singular integrals which gives rise to fully populated matrices, while the discretization of differential problems leads to sparse matrices and, above all, does not require the

TABLE VI: THE FIRST ORDER VOLUME-BASED FUNCTIONS SUBSET

The base of order $p = 1$ has twelve bubble functions

$$\underline{\boldsymbol{\Lambda}}^{B1} = \begin{bmatrix} \boldsymbol{\Lambda}^{B1}_{001} \\ \boldsymbol{\Lambda}^{B1}_{101} \\ \boldsymbol{\Lambda}^{B1}_{011} \\ \boldsymbol{\Lambda}^{B1}_{111} \end{bmatrix}, \qquad \underline{\boldsymbol{\Lambda}}^{B2} = \begin{bmatrix} \boldsymbol{\Lambda}^{B2}_{001} \\ \boldsymbol{\Lambda}^{B2}_{101} \\ \boldsymbol{\Lambda}^{B2}_{011} \\ \boldsymbol{\Lambda}^{B2}_{111} \end{bmatrix}, \qquad \underline{\boldsymbol{\Lambda}}^{B3} = \begin{bmatrix} \boldsymbol{\Lambda}^{B3}_{001} \\ \boldsymbol{\Lambda}^{B3}_{101} \\ \boldsymbol{\Lambda}^{B3}_{011} \\ \boldsymbol{\Lambda}^{B3}_{111} \end{bmatrix}$$

which in terms of the two array functions

$$\boldsymbol{M}(\eta, \xi_5) = \sqrt{210} \begin{bmatrix} \sqrt{\frac{5}{7}} \\ \sqrt{\frac{15}{7}}(2\eta - 1) \\ (6\xi_5 - 1) \\ \sqrt{3}(2\eta - 1)(6\xi_5 - 1) \end{bmatrix}, \qquad \boldsymbol{N}(\eta_1, \eta_2) = \sqrt{105} \begin{bmatrix} 1 \\ \sqrt{3}(2\eta_1 - 1) \\ \sqrt{3}(2\eta_2 - 1) \\ 3(2\eta_1 - 1)(2\eta_2 - 1) \end{bmatrix}$$

can be written in compact form as follows

$$\underline{\boldsymbol{\Lambda}}^{B1} = \boldsymbol{\Lambda}_{B1}\ \boldsymbol{M}(\eta_2, \xi_5), \qquad \underline{\boldsymbol{\Lambda}}^{B2} = \boldsymbol{\Lambda}_{B2}\ \boldsymbol{M}(\eta_1, \xi_5), \qquad \underline{\boldsymbol{\Lambda}}^{B3} = \boldsymbol{\Lambda}_{B3}\boldsymbol{N}(\eta_1, \eta_2);$$

$$\boldsymbol{\nabla} \cdot \underline{\boldsymbol{\Lambda}}^{B1} = (1 - 2\eta_1)\ \boldsymbol{M}(\eta_2, \xi_5), \quad \boldsymbol{\nabla} \cdot \underline{\boldsymbol{\Lambda}}^{B2} = (1 - 2\eta_2)\ \boldsymbol{M}(\eta_1, \xi_5), \quad \boldsymbol{\nabla} \cdot \underline{\boldsymbol{\Lambda}}^{B3} = (1 - 4\xi_5)\boldsymbol{N}(\eta_1, \eta_2)$$

The divergence of each bubble is proportional to one of the following scalar functions

$$(2\eta_1 - 1) = (\eta_1 - \eta_3), \qquad (2\eta_2 - 1) = (\eta_2 - \eta_4), \qquad (1 - 4\xi_5) = (1 - 4\xi_5),$$

$$\begin{aligned} &(2\eta_1 - 1)(2\eta_2 - 1) = (\eta_1 - \eta_3)(\eta_2 - \eta_4), \qquad && (2\eta_1 - 1)(1 - 4\xi_5) = (\eta_1 - \eta_3)(1 - 4\xi_5), \\ &(2\eta_2 - 1)(1 - 4\xi_5) = (\eta_2 - \eta_4)(1 - 4\xi_5), && (2\eta_1 - 1)(1 - 6\xi_5) = (\eta_1 - \eta_3)(1 - 6\xi_5), \\ &(2\eta_2 - 1)(1 - 6\xi_5) = (\eta_2 - \eta_4)(1 - 6\xi_5), \end{aligned}$$

$$\begin{aligned} &(2\eta_1 - 1)(2\eta_2 - 1)(1 - 6\xi_5) = (\eta_1 - \eta_3)(\eta_2 - \eta_4)(1 - 6\xi_5), \\ &(2\eta_1 - 1)(2\eta_2 - 1)(1 - 4\xi_5) = (\eta_1 - \eta_3)(\eta_2 - \eta_4)(1 - 4\xi_5) \end{aligned}$$

computation of integrals with singular kernels. (All this does not happen by chance, since the polynomials used in the construction of the hierarchical bases are precisely orthogonal with respect to *non-singular* weight functions.)

The volume-based functions proposed here are orthogonal for integrals on the volume of the pyramid, while the face-based function subsets are orthogonal only for integrals on the corresponding supporting face. However, as we did in [20], it is possible to make the face-based functions orthogonal also on the volume of the pyramid simply by adding to each of these a suitable linear combination of the volume-based functions. This has not been done in the present paper because it is not worth the trouble for the intended MoM applications, as just said. Instead, it remains of fundamental importance that the basis functions are not only independent, but also properly normalized; this is the main reason why we have used orthogonal polynomials to construct our divergence-conforming hierarchical bases.

For brevity and to avoid any loss of generality, we do not consider any integral equation; we rather establish that the degree of independence between the hierarchical basis functions of the pyramid is substantially similar to that of the basis functions for non-pyramidal cells by computing, as done in [12], the CN of the Gram matrices obtained using bases of different order on single straight cells, although admitting that to better assess the linear independence of the basis functions we should consider and study a large number of meshes, including hybrid ones that use curved cells. However, the advantage of doing as we do here is that the coefficients of the matrices we study are given by simple, non-singular 3D integrals on the child cell.

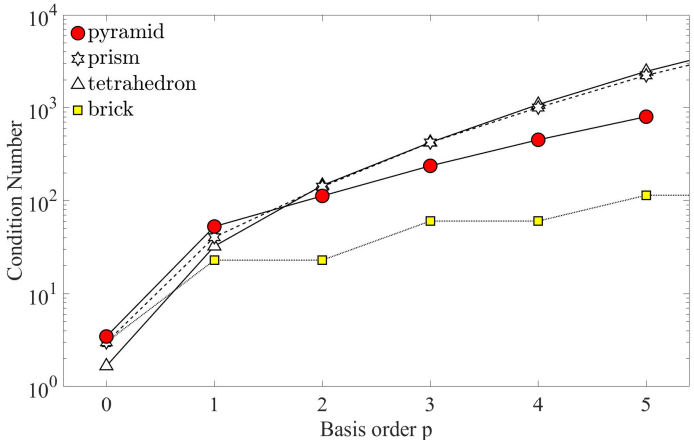

Fig. 3. The individual element Gram-matrix condition numbers grow exponentially with the order of the hierarchical base in use. The figure shows results obtained by considering differently shaped rectilinear cells whose edges have the same unitary length. The CNs for the other differently shaped equilateral elements of the same order are reported in [1, Chap. 5, Table 5.23].

Fig. 3 reports results for the individual element Gram-matrix condition numbers for hierarchical vector bases of different order obtained by considering *rectilinear* cells with equal edges and of unitary length. (Note that the CNs shown in

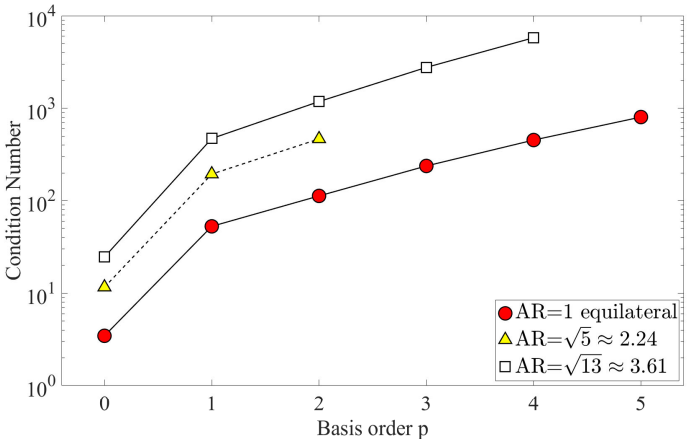

Fig. 4. Individual element Gram-matrix condition numbers for the rectilinear pyramids shown in Fig. 5, with Aspect Ratio AR=1 (equilateral), AR= $\sqrt{5}$, and AR= $\sqrt{13}$.

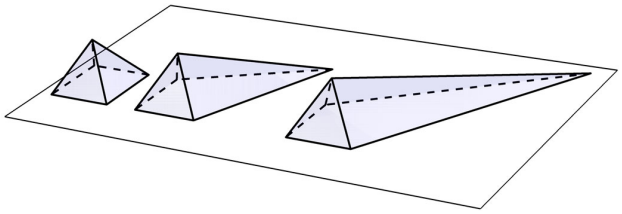

Fig. 5. The figure shows pyramids of different Aspect Ratio (AR) already studied in [12]: AR = 1 (equilateral) on the left, AR = $\sqrt{5}$ in the center, and AR = $\sqrt{13}$ on the right. The Jacobian $\mathcal{J}$ of the transformation from parent-to-child space is constant for an equilateral pyramid, while for distorted pyramids it can vary within the cell. For example, we have $\mathcal{J} = K$ for the pyramid shown on the left, while $\mathcal{J} = K(1+\eta_1+\eta_2)$ for the pyramid shown in the center, and $\mathcal{J} = K(1+2\eta_1+2\eta_2)$ for the pyramid shown on the right.

Fig. 3 do not depend on the cells edge-length in the child space since the unitary basis vectors and the Jacobian of the transformation from parent to child space are constant for the cells considered in Fig. 3.)

Fig. 4 compares the individual element mass-matrix condition numbers of the equilateral pyramid of Fig. 3 with those for pyramids obtained by moving one vertex of the base of the equilateral pyramid along its diagonal, doubling and tripling the length of this diagonal as depicted in Fig. 5. These pyramids have equal height and equal length for one of the diagonals of their base, but flat quadrilateral base of different shape. The ratio between the longest and the shortest side of each cell, commonly known as Aspect Ratio (AR), is given in the captions of Fig. 4 and 5. Note that unlike the equilateral pyramid, the distorted pyramids considered in Fig. 4 do not have a constant Jacobian. In view of the results of Fig. 4, we recommend using cells with AR near unity and less than 3 when using bases of order higher than the first.

In the end we find that for the pyramid the CN growth rate of the Gram matrix is not substantially worse than that of the hierarchical bases for other differently shaped cells (bricks, triangular prisms and tetrahedra).

VII. Conclusions

This paper presents a general very simple procedure to obtain higher order hierarchical divergence-conforming vector basis functions for pyramidal elements. The functions can be consistently used to deal with curvilinear elements and ensure the continuity of the normal vector component across adjacent elements of equal order but different shape. Properties of the vector basis functions are discussed in detail. The reported numerical results show that the degree of independence between the hierarchical basis functions of the pyramid is similar to that of the basis functions for the other non-pyramidal cells.

References

[1] R. D. Graglia, and A. F. Peterson, *Higher-order Techniques in Computational Electromagnetics,* SciTech Publishing/IET, Edison, NJ, 2016.

[2] J. C. Nédélec, "Mixed finite elements in R3," *Numer. Math.,* vol. 35, pp. 315–341, 1980.

[3] F.-X. Zgainski, J.-L. Coulomb, Y. Maréchal, F. Claeyssen, and X. Brunotte, "A new family of finite elements: the pyramidal elements," *IEEE Trans. Magn.*, vol. 32, no. 3, pp. 1393-1396, May 1996.

[4] J.-L. Coulomb, F.-X. Zgainski, and Y. Maréchal, "A pyramidal element to link hexahedral, prismatic and tetrahedral edge finite elements," *IEEE Trans. Magn.*, vol. 33, no. 2, pp. 1362-1365, Mar. 1997.

[5] R. D. Graglia, and I.-L. Gheorma, "Higher order interpolatory vector bases on pyramidal elements," *IEEE Trans. Antennas Propagat.*, vol. 47, no. 5, pp. 775-782, May. 1999.

[6] V. Gradinaru, R. Hiptmair, "Whitney elements on pyramids," *Electronic Transactions on Numerical Analysis,* Vol. 8, pp. 154-168, 1999.

[7] M. Bergot, G. Cohen, M. Duruflé, "Higher-order Finite Elements for hybrid meshes using new nodal pyramidal elements", *Journal of Scientific Computing,* Springer Verlag, vol. 42, No. 3, pp. 345-381, 2010. https://hal.archives-ouvertes.fr/hal-00454261

[8] N. Nigam, J. Phillips, "Numerical integration for high order pyramidal finite elements", *ESAIM: Mathematical Modelling and Numerical Analysis,* vol. 46, pp. 239, 2012.

[9] M. Bergot, M. Duruflé, "High-order optimal edge elements for pyramids, prisms and hexahedra," *Journal of Computational Physics,* vol. 232, Issue 1, pp. 189-213, Jan. 2013.

[10] F. Fuentes, B. Keith, L. Demkowicz, and S. Nagaraj, "Orientation embedded high order shape functions for the exact sequence elements of all shapes," *Computers & Mathematics with Applications,* vol. 70, pp. 353-458, 2015.

[11] A. Gillette, "Serendipity and tensor product affine pyramid Finite Elements," *The SMAI Journal of Computational Mathematics,* DOI: https://doi.org/10.5802/smai-jcm.14, Vol. 2, pp. 215-228, 2016.

[12] R. D. Graglia and P. Petrini, "Hierarchical curl-conforming vector bases for pyramid cells," in *IEEE Trans. Antennas Propagat.*, vol. 70, no. 7, pp. 5623-5635, July 2022, doi: 10.1109/TAP.2022.3145430.

[13] M. Benincasa, T. K. Sarkar, and others, *Parallel Scene Generation/Electromagnetic Modeling of Complex Targets in Complex Clutter and Propagation Environments,* AFRL-SN-RS-TR-2005-365, Final Technical Report, October 2005 (please see also https://books.google.it/books?id=Ypn8jwEACAAJ).

[14] M. Salazar-Palma, T. K. Sarkar, L.-E. Garcia-Castillo, T. Roy, and A. Djordjevic, *Iterative and Self-Adaptive Finite-Elements in Electromagnetic Modeling*. Boston, Artech House. 1998.

[15] L. Demkowicz, *Computing with hp-Adaptive Finite Elements*, vol. 1 Boca Raton, Chapman & Hall/CRC, 2007.

[16] L. Demkowicz, J. Kurtz, D. Pardo, M. Paszenski, W. Rachowicz, A. Zdunek, *Computing with hp-Adaptive Finite Elements*, vol. 2 Boca Raton, Chapman & Hall/CRC, 2008.

[17] R. D. Graglia, A. F. Peterson, and F. P. Andriulli, "Curl-Conforming hierarchical vector bases for triangles and tetrahedra," *IEEE Trans. Antennas Propagat.*, vol. 59, no. 3, pp. 950-959, Mar. 2011.

[18] R. D. Graglia, and A. F. Peterson, "Hierarchical curl-conforming Nedelec elements for quadrilateral and brick cells," *IEEE Trans. Antennas Propagat.*, vol. 59, no. 8, pp. 2766-2773, Aug. 2011.

[19] R. D. Graglia, and A. F. Peterson, "Hierarchical curl-conforming Nedelec elements for triangular-prism cells," *IEEE Trans. Antennas Propagat.*, vol. 60, no. 7, pp. 3314-3324, Jul. 2012.

[20] R. D. Graglia, and A. F. Peterson, "Hierarchical divergence-conforming Nédélec elements for volumetric cells," *IEEE Trans. Antennas Propagat.*, vol. 60, no. 11, pp. 5215-5227, Nov. 2012.

[21] S. M. Rao, D. R. Wilton, and A. W. Glisson, "Electromagnetic scattering by surfaces of arbitrary shape," *IEEE Trans. Antennas Propagat.*, vol. 30, no. 3, pp. 409-418, May 1982.

[22] R. D. Graglia, D. R. Wilton, and A. F. Peterson, "Higher order interpolatory vector bases for computational electromagnetics," *IEEE Trans. Antennas Propagat.*, vol. 45, no. 3, pp. 329-342, March 1997, doi: 10.1109/8.558649.

[23] R. D. Graglia, "Hierarchical vector bases for pyramid cells," Proc. of the *2022 International Conference on Electromagnetics in Advanced Applications (ICEAA)*, pp. 406-407, Cape Town, South Africa, Sept. 5-9, 2022.